Motion-Enhanced Peripheral Color Discrimination in VR: Interactions with Crowding and Speed

Yuyang Cai
University of Technology Sydney
Sydney, Australia
Yuyang.Cai@student.uts.edu.au

Charlie Li-Ting Tsai
University of Technology Sydney
Sydney, Australia
Li-Ting.Tsai@uts.edu.au

Juno Kim
University of New South Wales
Sydney, Australia
juno.kim@unsw.edu.au

Eva Cheng
University of Technology Sydney
Sydney, Australia
Eva.Cheng@uts.edu.au

Stuart Perry
University of Technology Sydney
Sydney, Australia
Stuart.Perry@uts.edu.au

ABSTRACT

Peripheral color perception in VR is challenged when motion, crowding, and eccentricity interact, yet their combined effects remain poorly understood. We conducted a within-subjects color-matching study in a head-mounted display (Meta Quest Pro; $N = 20$), crossing motion (static, 5, 8 rad/s), eccentricity (10°, 30°), and crowding (4:4 vs. 1:6 target:distractor) under eye-tracked fixation. Moderate oscillatory motion (5–8 rad/s) robustly improved performance, reducing hue error (Δh) by 40–43% and total color difference (ΔE, CIEDE2000) by ∼30%, while crowding had no significant effect. A pronounced Motion×Eccentricity interaction revealed a chroma-bias reversal: chroma was overestimated at 10° and underestimated at 30° during static viewing, whereas motion flipped this pattern. These findings fill a key gap in dynamic peripheral color perception for VR and suggest actionable design guidance: moderate motion can support color-critical peripheral elements, and rendering pipelines should apply motion- and eccentricity-aware chroma compensation.

CCS CONCEPTS

• **Human-centered computing** → **Virtual reality**.

ACM Reference Format:
Yuyang Cai, Charlie Li-Ting Tsai, Juno Kim, Eva Cheng, and Stuart Perry. 2025. Motion-Enhanced Peripheral Color Discrimination in VR: Interactions with Crowding and Speed. In *SIGGRAPH Asia 2025 Technical Communications (SA Technical Communications '25), December 15–18, 2025, Hong Kong, Hong Kong*. ACM, New York, NY, USA, 4 pages. https://doi.org/10.1145/3757376.3771416

1 INTRODUCTION

Accurate peripheral color perception is essential in VR (e.g., simulation training), where users must interpret color-coded alerts while simultaneously performing central tasks [Vater et al. 2022]. In head-mounted displays (HMDs), limited field-of-view, visual crowding, and object motion can markedly degrade peripheral color discrimination—potentially leading to critical errors in high-stakes contexts [Koulieris et al. 2019; Strasburger et al. 2011; Whitney and Levi 2011]. VR further challenges perception because multiple visual streams at different eccentricities must be processed within a confined display, under continual head and scene dynamics. Unlike traditional 2D displays, VR tightly couples spatial, motion, and color cues, yet most prior work emphasizes static or central vision; the joint effects of motion, crowding, and eccentricity remain underexplored [Clay et al. 2019; Duinkharjav et al. 2022; Levi 2008].

Motion modulates peripheral color via temporal integration mechanisms. Oscillatory stimuli can enhance chromatic discrimination by engaging temporal sensitivity peaks that favor moderate rates [Kelly 1983; Tyler and Hamer 1990]. In VR, however, motion can also mask changes—"motion silencing"—when features update during movement [Suchow and Alvarez 2011]. Consequently, whether motion improves or impairs hue error (Δh) and chroma error (ΔC) likely depends on viewing dynamics and task timing.

The full three-way interaction of motion, crowding, and eccentricity in VR has not been systematically tested. We therefore conducted a within-subjects color-matching study on Meta Quest Pro, varying eccentricity (10°, 30°), crowding (4:4 vs. 1:6), and motion (static, 5, 8 rad/s), with real-time eye tracking enforcing fixation to isolate peripheral processing. Reporting LCh errors (ΔC, Δh, ΔE), we show: (1) moderate motion robustly improves hue discrimination and overall accuracy, and (2) a motion–eccentricity interaction in chroma flips bias between 10° and 30°, providing concrete targets for adaptive, perception-aware VR rendering.

2 METHODS

2.1 Apparatus and Display Calibration

The study was implemented in Unity 2022.3 and presented on a Meta Quest Pro HMD (90 Hz; 1800×1920 per eye). Stimuli used unlit shaders on a mid-gray background at fixed device brightness. A Quest Touch controller was used for responses.

To ensure device-referred color accuracy, we profiled the HMD with a tristimulus colorimeter positioned at the eye-box and measured the per-channel luminance response and primaries. Measured primaries and white were used to derive an RGB→XYZ matrix under the headset's native white (near D65), followed by XYZ→CIELAB; RGB drives were gamma-linearized before conversion. All reported ΔE (CIEDE2000), Δh, and ΔC were computed

SA Technical Communications '25, December 15–18, 2025, Hong Kong, Hong Kong

ACM ISBN 979-8-4007-2136-6/2025/12
https://doi.org/10.1145/3757376.3771416

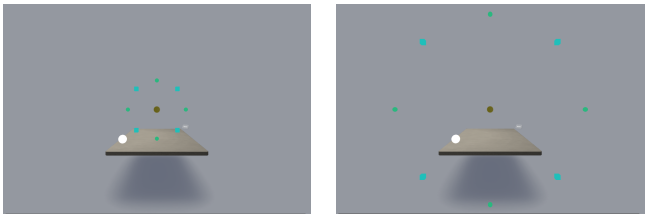

Figure 1: Eccentricity conditions at 10° (a) and 30° (b) under low crowding (4 targets + 4 jammers). Spheres = targets; cubes = jammers; yellow–green = fixation; white = matching feedback. Items lie on an iso-eccentric ring ($r = d \tan\theta$, $d = 1.5$ m); apparent size is constant.

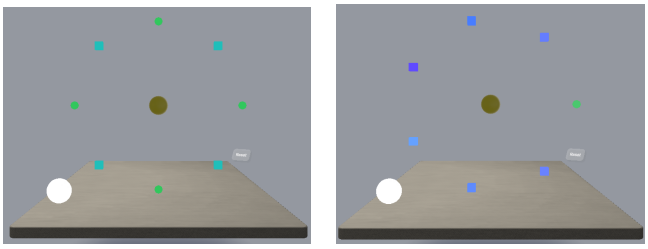

Figure 2: Crowding configurations on the iso-eccentric ring: (a) low (4:4) and (b) high (1:6). All stimuli maintain constant visual angle.

from these device-referred CIELCh values. Room illumination was dim and constant; all participants used the same headset.

2.2 Stimuli and Design

The virtual scene comprised a neutral gray room, a yellow–green fixation sphere above a desk, and a white reference sphere that mirrored ColorBar selections during matching. Spherical *test balls* (targets) and cubic *jammers* (distractors) were placed on iso-eccentric rings centered at fixation at 10° or 30°. Ring radius followed $r = d \tan\theta$ (d=1.5 m). Apparent object size (visual angle) and angular spacing were held constant across eccentricities.

We used a fully within-subjects 2×2×3 design with factors: **Eccentricity** (10°, 30°), **Crowding** (low 4:4 vs. high 1:6), and **Motion** (static, 5, 8 rad/s), yielding 12 conditions. Each condition was repeated three times (36 trials/participant). In both crowding levels, exactly one test ball (sphere) served as the color-matching target; all cubes were jammers. Item positions on the ring and the target's initial angular position were randomized per trial with minimum spacing to avoid overlap. Condition order was block-randomized and counterbalanced across participants.

2.2.1 Motion parameterization. In motion trials, the entire set (target+distractors) oscillated rigidly about fixation:

$$\theta(t) = \theta_0 + A\sin(\omega t),$$

with amplitude $A = 30°$ and $\omega \in \{5, 8\}$ rad/s (temporal frequencies $\approx \{0.80, 1.27\}$ Hz). For a given eccentricity, all items moved synchronously along the circular path; spatial parameters (amplitude, radius, trajectory) were identical across the two motion speeds.

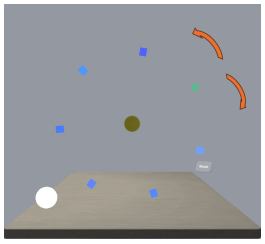

Figure 3: Rigid oscillation about fixation at 5 or 8 rad/s with ±30° (example shown for high crowding).

Figure 4: ColorBar with 56 patches at fixation for matching the cued final color.

2.3 Eye-Tracking Fixation Control

Binocular gaze was obtained by averaging left/right rays from Unity `OVREyeGaze`. Fixation was monitored at 2 Hz (every 0.5 s): for each sample we intersected the binocular ray with the stimulus plane at fixation depth and computed (i) position deviation (m) to fixation, (ii) directional deviation (°) between gaze direction and the eye-to-fixation vector, and (iii) gaze-point speed (m/s). A sample was flagged off-fixation if position deviation >0.20 m (≈7.6° at 1.5 m) or directional deviation >5°. Thresholds were chosen to remain below the minimum target eccentricity and to accommodate natural fixational movements during the 6.2 s presentation.

Eye-tracking was used for quality control only: trials were not interrupted online and no trials were excluded based on eye data. As a limitation, 2 Hz sampling may miss brief saccades; however, the long presentation and strict instructions reduce the likelihood of sustained foveation of the peripheral target.

2.4 Procedure

Each trial began with a 50 ms fixation, followed by a scripted 6.2 s color sequence in which objects transitioned slowly and then rapidly to a final color. An audio cue marked the final phase and indicated the moment to be matched. After offset, a ColorBar appeared at fixation for matching.

2.4.1 Color matching interface (ColorBar). The ColorBar comprised 56 pre-defined patches (0.5°×0.5°) on a neutral gray background. The set was curated in pilots to ensure peripheral separability under static/motion conditions; each patch had a unique device-referred RGB mapping to a distinct CIELCh value. Participants navigated with the controller and confirmed selections by button press.

2.5 Measures and Analysis

Selections were converted to CIELCh. We computed chroma error ΔC, hue error Δh (deg), and total color difference ΔE (CIEDE2000). Within-subjects effects of Motion (3), Eccentricity (2), and Crowding (2) were tested with an Aligned Rank Transform three-way repeated-measures ANOVA (ART). Significant effects were followed by Holm-adjusted pairwise comparisons using estimated marginal means (*emmeans*). We report condition means with 95% confidence intervals. (Implementation: `ARTool`/`emmeans` in R.)

2.6 Participants

Twenty adults (aged 20–30 years) with normal or corrected-to-normal vision and normal color perception (Ishihara) participated. All provided informed consent. The study was approved by the institutional human research ethics committee.

3 RESULTS

Participant responses were converted to CIELCh coordinates. Three error metrics were computed for each condition: chroma error (ΔC), hue error (Δh), and total color difference (ΔE; CIEDE2000). Data were analyzed using the Aligned Rank Transform (ART) procedure for non-parametric three-way repeated-measures ANOVA, assessing main and interaction effects of motion (static, 5rad/s, 8rad/s), eccentricity (10°, 30°), and crowding (low, high). Significant effects were followed by Holm-adjusted [Holm 1979] pairwise comparisons using estimated marginal means (emmeans). Eye-tracking data were recorded only to ensure fixation compliance and were not included in the statistical analysis. Results are reported as means with 95% confidence intervals.

3.1 Motion Effects

Motion significantly enhanced color perception accuracy. While ΔC showed no significant main effect ($F(2, 209) = 2.00$, Holm $p = .825$), both Δh and ΔE demonstrated substantial improvements under motion conditions. Hue error (Δh) decreased significantly ($F(2, 209) = 33.73$, Holm $p < .001$) from 15.0 [13.5, 16.5] in static viewing to 8.5 [7.5, 9.5] at 5rad/s and 9.0 [8.0, 10.0] at 8rad/s, representing approximately 43% and 40% improvements, respectively.

Total color error (ΔE) similarly decreased significantly ($F(2, 209) = 25.28$, Holm $p < .001$) from 10.0 [9.2, 10.8] under static conditions to 7.0 [6.2, 7.8] at both motion frequencies (~30% improvement). Post-hoc analyses confirmed significant differences between static and both motion conditions (all $p < .01$), with no significant difference between 5rad/s and 8rad/s.

3.2 Eccentricity Effects

Eccentricity showed limited effects across color perception measures. ΔC ($F(1, 209) = 0.52$, Holm $p = 1.000$) and ΔE ($F(1, 209) = 0.19$, Holm $p = 1.000$) remained unaffected by eccentricity. Δh showed a marginal trend ($F(1, 209) = 6.50$, Holm $p = 0.069$) toward higher hue errors at greater eccentricity, but failed to reach significance after correction.

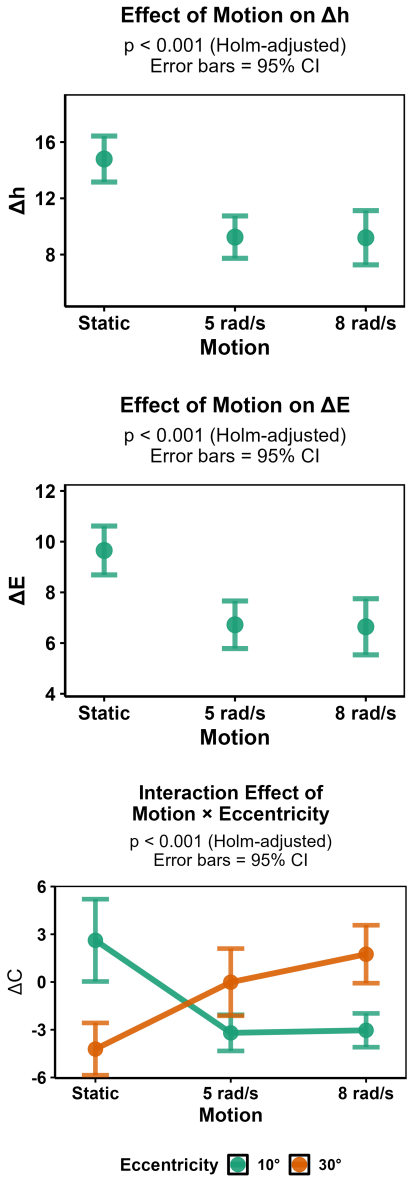

Figure 5: Significant effects of motion: (a) motion reduced hue error (Δh); (b) motion reduced total color difference (ΔE); (c) motion×eccentricity reversed chroma error (ΔC). Holm-adjusted $p < .001$.

3.3 Crowding Effects

Crowding density produced no significant main effects on color perception. ΔC ($F(1, 209) = 0.01$, Holm $p = 1.000$) and Δh ($F(1, 209) = 2.05$, Holm $p = 0.768$) showed no significant differences between crowding conditions. ΔE showed a non-significant trend ($F(1, 209) = 3.68$, Holm $p = 0.340$) toward lower errors under high crowding.

3.4 Motion × Eccentricity Interaction

A highly significant interaction emerged for ΔC ($F(2, 209) = 37.39$, Holm $p < .001$), revealing a motion-induced reversal of center–periphery chromaticity bias. Under static viewing, participants overestimated chroma at 10° (mean +3.0, 95% CI [2.0, 4.0]) while underestimating it at 30° (mean −4.0, 95% CI [−5.0, −3.0]). With motion, this bias flipped: at 5rad/s, 10° showed underestimation (mean −3.0, 95% CI [−4.0, −2.0]) and 30° showed overestimation (mean +1.0, 95% CI [0.0, 2.0]). At 8rad/s the same reversal was observed ($10° \approx -3$, $30° \approx +2$; Fig. 5 (c)).

No other interactions reached significance: Motion×Crowding (ΔC, Δh Holm p=1.000; ΔE p=0.414), Eccentricity×Crowding (all p=1.000), and Motion×Eccentricity×Crowding (all p=1.000).

4 DISCUSSION

The results demonstrate that oscillatory motion at 5rad/s and 8rad/s enhances peripheral color discrimination in VR environments, reducing hue error (Δh) by approximately 40–43% (from 15° to 8.5°–9.0°) and total color difference (ΔE) by ∼30% (from 10.0 to 7.0 CIEDE2000 units) compared to static conditions. These improvements exceed the $\Delta E = 3$ threshold for meaningful perceptual differences and correspond to established temporal sensitivity peaks in human vision, where moderate frequencies enhance chromatic processing [Kelly 1983; Tyler and Hamer 1990]. Both oscillation frequencies showed comparable effects, suggesting robust engagement of motion-dependent enhancement mechanisms that do not require precise frequency-specific optimization [Bowen et al. 1989]. The lack of significant motion effects on chroma difference (ΔC) indicates processing selectivity, where oscillatory motion benefits are limited to hue-dependent tasks[Van den Berg et al. 2007]. Our motion-enhancement finding may seem at odds with "motion silencing" [Suchow and Alvarez 2011], which impairs detection of transient feature changes during motion. However, motion silencing concerns change detection, whereas our task required reproducing a color sampled at a cued moment after a sustained 6.2 s presentation. Under sustained viewing, temporal integration can improve chromatic encoding even as motion reduces moment-to-moment change awareness.

The motion × eccentricity interaction on ΔC shows a systematic bias reversal with implications for VR calibration: at 10° a static overestimation (+3.0) flips to underestimation with motion, whereas at 30° a static underestimation (−4.0) becomes overestimation (+1.0 [0.0, 2.0] at 5rad/s, ∼+2 at 8rad/s). This pattern indicates that eccentricity effects are motion-dependent in VR: differences in peripheral temporal sensitivity with eccentricity make oscillatory motion flip perceived chroma bias [Kelly 1983; Strasburger et al. 2011; Tyler and Hamer 1990]. This quantifiable reversal refines static peripheral-vision accounts for dynamic VR contexts [Bouma 1970; Strasburger et al. 2011] and supports eccentricity-specific chroma compensation in rendering pipelines. These findings establish oscillatory stimulus motion as a practical enhancement parameter for VR color processing with minimal computational overhead. Study limitations include modest sample size ($N = 20$), limited eccentricity range that may not capture extreme peripheral effects, and restricted motion frequency sampling that limits optimal parameter identification.

5 CONCLUSIONS

This study examined peripheral color perception in VR when motion, crowding, and eccentricity interact. Oscillatory motion at 5–8 rad/s substantially improved performance, reducing hue error by 40–43% and ΔE (CIEDE2000) by ∼30%. We also observed a robust motion×eccentricity chroma-bias reversal (10° vs. 30°), challenging assumptions based on static peripheral color perception. With eye-tracked fixation under realistic HMD viewing, these results fill a key gap on dynamic peripheral color. They offer actionable guidance: moderate motion can support color-critical peripheral cues, and rendering pipelines should apply motion- and eccentricity-aware chroma compensation. Our findings provide evidence that controlled motion can mitigate peripheral color limits in head-mounted displays and motivate adaptive, perceptually optimized VR rendering strategies.

REFERENCES

Herman Bouma. 1970. Interaction effects in parafoveal letter recognition. *Nature* 226, 5241 (1970), 177–178.

Richard W Bowen, Joel Pokorny, and Vivianne C Smith. 1989. Sawtooth contrast sensitivity: decrements have the edge. *Vision research* 29, 11 (1989), 1501–1509.

Viviane Clay, Peter König, and Sabine Koenig. 2019. Eye tracking in virtual reality. *Journal of Eye Movement Research* 12, 1 (2019), 1–10.

Budmonde Duinkharjav, Kenneth Chen, Abhishek Tyagi, Jiayi He, Yuhao Zhu, and Qi Sun. 2022. Color-perception-guided display power reduction for virtual reality. *ACM Transactions on Graphics (TOG)* 41, 6 (2022), 1–16.

Sture Holm. 1979. A Simple Sequentially Rejective Multiple Test Procedure. *Scandinavian Journal of Statistics* 6, 2 (1979), 65–70.

DH Kelly. 1983. Spatiotemporal variation of chromatic and achromatic contrast thresholds. *Journal of the Optical Society of America* 73, 6 (1983), 742–750.

George Alex Koulieris, Kaan Akşit, Michael Stengel, Rafał K Mantiuk, Katerina Mania, and Christian Richardt. 2019. Near-eye display and tracking technologies for virtual and augmented reality. *Computer Graphics Forum* 38, 2 (2019), 493–519.

Dennis M Levi. 2008. Crowding—An essential bottleneck for object recognition: A mini-review. *Vision research* 48, 5 (2008), 635–654.

Hans Strasburger, Ingo Rentschler, and Martin Jüttner. 2011. Peripheral vision and pattern recognition: A review. *Journal of Vision* 11, 5 (2011), 13–13.

Jordan W Suchow and George A Alvarez. 2011. Motion silences awareness of visual change. *Current Biology* 21, 2 (2011), 140–143.

Christopher W Tyler and Russell D Hamer. 1990. Analysis of visual modulation sensitivity. IV. Validity of the Ferry–Porter law. *Journal of the Optical Society of America A* 7, 4 (1990), 743–758.

Ronald Van den Berg, Jos BTM Roerdink, and Frans W Cornelissen. 2007. On the generality of crowding: Visual crowding in size, saturation, and hue compared to orientation. *Journal of Vision* 7, 2 (2007), 14–14.

Christian Vater, Benjamin Wolfe, and Ruth Rosenholtz. 2022. Peripheral vision in real-world tasks: A systematic review. *Psychonomic bulletin & review* 29, 5 (2022), 1531–1557.

David Whitney and Dennis M Levi. 2011. Visual crowding: A fundamental limit on conscious perception and object recognition. *Trends in Cognitive Sciences* 15, 4 (2011), 160–168.